

Surface Supercooling and Stability of *n*-Alkane Films

Nobuo Maeda* and Vassili V. Yaminsky

*Department of Applied Mathematics, Research School of Physical Sciences and Engineering,
Australian National University, Canberra ACT 0200, Australia*

(Received 16 August 1999)

The surface tension of *n*-octadecane was studied in the vicinity of the bulk melting point using both the maximum bubble pressure and Wilhelmy plate methods. The bubble surfaces were found to be supercooled below the surface freezing point. The onset of surface freezing is indicated by a sharp drop in surface tension at a constant temperature. This transition is accompanied by an increased film stability resulting in longer bubble lifetimes at the liquid surface. Variations in bubble lifetime reflect changes in the interfacial mechanical properties of the film from liquidlike to solidlike.

PACS numbers: 68.10.Cr, 64.70.Dv, 68.15.+e

It has recently been reported that long chain *n*-alkanes exhibit the phenomena of surface freezing, whereby the surface monolayer of a melt remains solidlike up to 3 °C above the bulk melting point (T_m). The physical properties of this new surface phase are as yet not understood but may have implications for several other classes of molecules. Surfactants, lipids, and liquid crystals as well as molecules that can exhibit self-assembly, such as the alkanethiols and alkanolic acids, all contain structural units of *n*-alkanes. As such, a greater understanding of the surface behavior of *n*-alkanes is essential.

Surface tension (γ) measurements first revealed that liquid *n*-alkanes undergo a two-dimensional phase transition at the vapor interface [1,2]. This has subsequently been confirmed with other techniques including x-ray [2,3], nonlinear optics [4], and ellipsometry [5]. The monotonic increase in γ as the temperature is lowered [6] breaks a few degrees above T_m , where γ shows a maximum [1,2]. At this surface freezing point (T_{sf}), the values of surface excess entropy and the surface latent heat change from positive to negative ($S = -\partial\gamma/\partial T < 0$, $L = -T\partial\gamma/\partial T < 0$). X-ray studies have revealed formation of a hexagonally ordered monolayer in which the molecules are oriented normal to the surface of the liquid [2,3].

It has been recently realized that these surface frozen monolayers have mechanically solidlike properties as well. Pure (one-component) *n*-eicosane was found to form stable foams after shaking the liquid below T_{sf} [7].

A number of studies on static aspects of surface freezing of *n*-alkanes have been carried out [1–5,8]. However, the dynamics of surface freezing remain largely unexplored. There is currently great interest in the supercooling and nucleation in alkanes and polymers and the role of the surface crystallization is suggested to play a major role [9].

In this Letter we report on the dynamic surface properties of *n*-octadecane using the maximum bubble pressure (MBP) method and compare the results with those using the static Wilhelmy plate (WP) method. We present new evidence showing that surface freezing requires supercooling and confirm that the mechanical properties of the surface changes from liquidlike to solidlike upon surface

freezing. Our results suggest occurrence of supercooling of the monolayer itself.

n-octadecane was purchased from Aldrich (purity >99%), and distilled under reduced pressure. Prior to each experiment, the liquid surface was aspirated with a clean Pasteur pipette. WP measurements were carried out in a temperature controlled and sealed chamber, using P_2O_5 as a drying agent. Basic principles of the static Wilhelmy plate method are described elsewhere [10]. Filter paper was used as the porous plate to ensure complete wetting. Filter paper is commonly used as a standard Wilhelmy plate in the Langmuir trough. In previous surface freezing studies [3,5] it has been shown to give the same results as a roughened platinum plate. The measured weight of the plate initially increased due to wetting by the liquid. Following equilibration, the temperature was changed continuously while the weight was recorded simultaneously. The added weight of the wetted filter paper prevents absolute measurements of γ with this method. Rather, relative values of γ were measured and put in correspondence with known values of γ at temperatures above T_{sf} .

Basic principles of the MBP method are described in standard textbooks [10]. A U-shaped glass capillary was used, resulting in bubbles being released from the upwardly oriented capillary orifice. Dry nitrogen gas was purged through the capillary and the bubble pressure was recorded simultaneously with images of the bubbles, using a video microscope. The chamber was temperature controlled but left unsealed to avoid a buildup of pressure inside the chamber. The gas flow was controlled by a two-stage valve, and the rate of gas supply was monitored by a flowmeter. The gas was passed through a copper tube heat exchanger (volume \approx 2.5 ml) that was maintained at the temperature of the chamber, before entering the capillary. The temperature of nitrogen gas entering the heat exchanger was \sim 17–20 °C. The total volume between the capillary orifice and the valve was approximately 3 ml. The capillary size was calibrated using distilled ethanol ($\gamma = 22.32$ mN/m at 20 °C). The inner diameter of the capillary orifice measured this way

was $62 \mu\text{m}$. Measurements at different depths allowed calibration of the pressure sensor and a check for the hydrostatic pressure correction. The temperature was scanned at approximately $0.05 \text{ }^\circ\text{C}/\text{min}$ and monitored within $\pm 0.05 \text{ }^\circ\text{C}$. In the results shown below “cooling1” and “cooling2” measurements were carried out while the temperature was monotonically lowered until the bulk freezing took place, whereas for “cycle1” and “cycle2” the temperature was reversed while the bulk remained supercooled.

Results of $\gamma(T)$ measured by the MBP method in the vicinity of T_m for four typical experiments are shown along with data obtained by the WP method in Fig. 1. These four experiments were carried out using the same

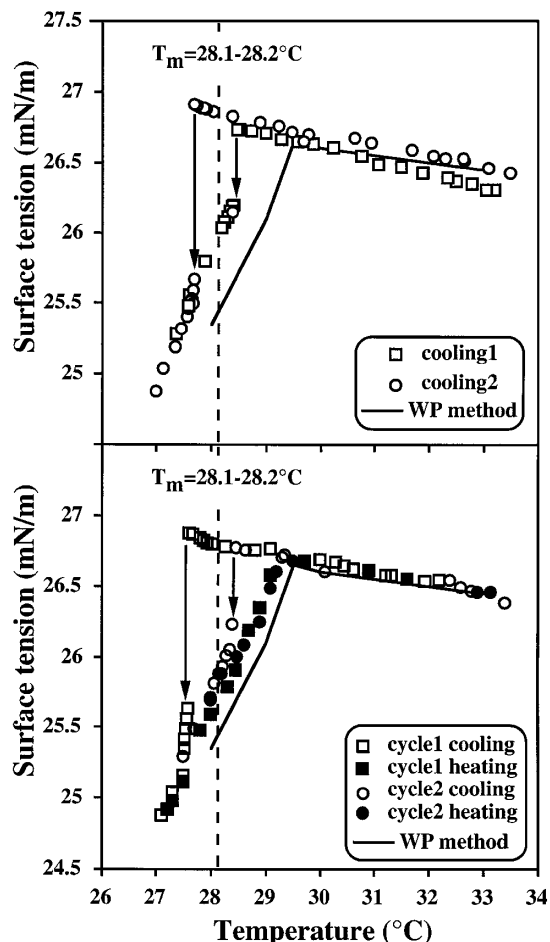


FIG. 1. Surface tension versus temperature measured by the MBP method and the WP method. The two sets of data in the top figure are for cooling only, whereas the bottom figure shows cooling (open symbols) and heating (filled symbols) cycles. Surface tension values measured by the MBP method gradually increase upon cooling, showing no immediate break in the trend at the surface freezing temperature. This corresponds to a metastable liquid surface. The thermodynamically stable solid surface phase shows different temperature dependence, as is shown by the WP data over this temperature range. Over the rest of the cycles both methods give the same results. The process of surface solidification possesses hysteresis characteristic of a first order bulk phase transition.

sample of liquid in the following order; cooling1, cooling2, cycle1, and cycle2. The $\gamma(T)$ data obtained using the WP method exhibits a change of slope at T_{sf} , as reported previously. The MBP method on cooling reveals a continued increase in γ below the T_{sf} , followed by a sharp decrease in γ as the surface freezes. The associated pressure drop (release of an excess pressure) is completed within 30 sec, and occurs with a negligible temperature change. During this period the measured pressure does not necessarily reflect true γ values, and they were therefore discarded. Instead the transition is indicated with arrows in Fig. 1. The temperature at which this transition occurs is not repeatable (above or below T_m) in these experiments, even when measurements are done using the same lot of liquid. For example, data in Fig. 1 show no correlation between the transition temperature and sequence order of experimental run, indicating there was no long term effect of accumulation of contaminants in the system. No correlation between the transition temperature and bubbling rate over the range studied (2 to 6 sec per bubble) was observed. Thereafter, γ continuously decreases as the temperature is lowered until bulk freezing takes place. The increase of γ on subsequent heating continues until T_{sf} is reached, and the trend of γ obtained is independent of the method employed.

The lifetimes of bubbles produced at the capillary and allowed to rise to the bulk liquid-air interface are shown as a function of temperature in Fig. 2. Three distinct regions of bubble lifetimes are observed. From above to slightly below T_{sf} , the bubbles immediately burst when they reach the surface. The coalescence time is less than 20 ms, which is the time resolution of our video camera (we refer to this region as A). At some temperature below T_{sf} , but before the sudden drop in γ is observed, the coalescence behavior suddenly changes. Some bubbles persist at the surface for a few seconds before bursting. The percentage of bubbles that persist is initially about 20%, and steadily increases as the temperature is further lowered (we refer to this region as B). At the temperature at which the drop in γ is observed, the majority of the bubbles become stable, and their lifetime at the surface increases to several minutes (we refer to this region as C). It is possible to observe the bubbles down to approximately $1 \text{ }^\circ\text{C}$ below T_m , where the supercooled bulk liquid in the cell begins to freeze. On subsequent heating, the bubbles remain stable at the surface until approximately $0.2 \text{ }^\circ\text{C}$ below T_{sf} . At this temperature the bubbles become unstable and burst in less than 20 ms thereafter. The hysteresis in bubble lifetimes closely correlates to supercooling detected via surface tension measurements in Fig. 1.

The lifetime of a bubble at the surface reflects the stability of the liquid film between the two gas phases. This is determined first by the thinning of the film and then by film bursting due to surface waves. It is known that viscous flow of a fluid near a solid wall exhibits a velocity gradient due to the nonslip boundary condition. However, this does not apply to a pure liquid-vapor interface where interfacial slip readily occurs. This explains the short bubble

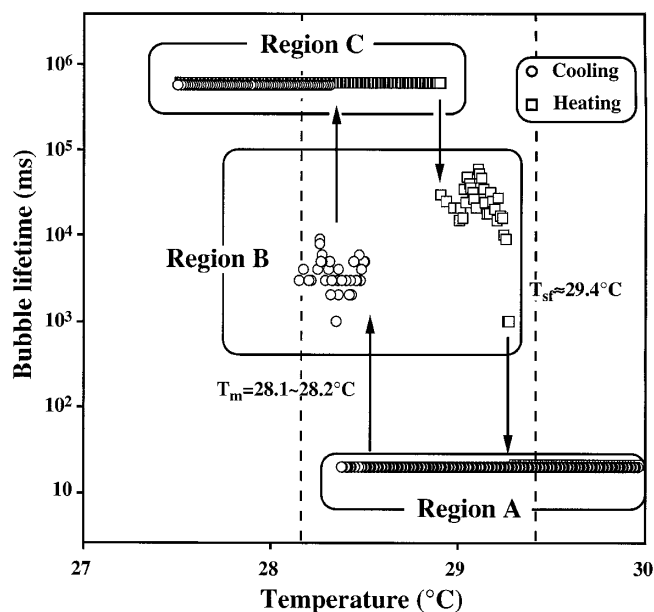


FIG. 2. Lifetime of individual bubbles as a function of temperature (data for cycle2 of Fig. 1). On cooling (open circle), the lifetime first increases from milliseconds (region A) to seconds (region B) at a temperature below T_{sf} , then to minutes or more (region C) after release of the surface supercooling. On heating (open square), the bubbles remain stable up to approximately 0.2°C below T_{sf} . The lifetime of the bubbles drops sharply to less than 20 ms at this temperature. The minimum time resolution was 20 ms and maximum observation time was 10 min. The hysteresis in bubble lifetimes closely correlates to supercooling detected via surface tension measurements in Fig. 1.

lifetimes typically observed in pure liquids. When neither surface is frozen, the film drains rapidly (region A). When one of the surfaces is frozen, the mechanism of the film drainage changes from dynamic to viscosity controlled. It takes longer for the film to drain to submicron thickness at which it becomes unstable (region B). Since it is unlikely that all the surface of the liquid in the cell freezes at the same time, the steady increase in the percentage of longer living bubbles observed may be a result of an increase in the fraction of the bulk interface that is frozen. A small liquid region in the frozen monolayer may well reduce bubble lifetime, as this will increase both film drainage and the probability of film rupture due to surface waves. When both surfaces are frozen, the film drainage time becomes even longer (region C). Our results qualitatively confirm the earlier study, where lifetimes of the *n*-eicosane foams are observed to increase from ≈ 5 sec above T_{sf} to ≈ 12 sec below T_{sf} [7]. However, we observe a more distinct difference between the two surface states.

A notable feature of these observations is that the surface supercooling shown by the MBP method does not occur at the interface probed with the Wilhelmy plate. It has been suggested that surface nucleation requires a sufficient density of nucleation sites, from the observation that surface freezing does not always occur in the absence of a

Wilhelmy plate [3]. It has also been suggested that impurities are necessary to provide nucleation sites for surface freezing, though the actual nature of the impurities seems to be unimportant [3]. Therefore, these effects might explain why the WP method does not show surface supercooling. In the MBP method, the surface lifetime is orders of magnitude shorter and the liquid surface does not remain stagnant as it does in the WP method. Moreover, the probability of surface nucleation, which is proportional to the surface area, is here much smaller. So a bubble can be supercooled easily. However, once one bubble freezes, it may leave some nucleation sites inside the capillary when it detaches. The neck that connects the bubble to the capillary becomes thinner and finally breaks when the bubble detaches. Then a small portion of the surface of the former frozen bubble can be inherited to the subsequent one. Thus once surface nucleation occurs for one of the bubbles, the process may continue autocatalytically. Subsequent bubbles have little trouble in nucleation.

In summary, the surface of the bubbles is supercooled below T_{sf} . The onset of surface freezing is reflected in a sharp drop in γ . The transition is accompanied by an increased film stability against bubble coalescence, in which the mechanical properties of both the liquid-air interface and the liquid-bubble interface changes from liquidlike to solidlike.

We thank H. K. Christenson and Vince Craig for helpful discussion, T. Sawkins and A. Hyde for technical assistance, and J. Derlacki for distillation of *n*-octadecane.

*Corresponding author.

Electronic address: nmall0@rsphysee.anu.edu.au

- [1] J. C. Earnshaw and C. J. Hughes, *Phys. Rev. A* **46**, 4494 (1992).
- [2] X. Z. Wu, E. B. Sirota, S. K. Sinha, B. M. Ocko, and M. Deutsch, *Phys. Rev. Lett.* **70**, 958 (1993); X. Z. Wu, B. M. Ocko, E. B. Sirota, S. K. Sinha, M. Deutsch, B. H. Cao, and M. W. Kim, *Science* **261**, 1018 (1993); X. Z. Wu, B. M. Ocko, E. B. Sirota, S. K. Sinha, and M. Deutsch, *Physica (Amsterdam)* **200A**, 751 (1993).
- [3] B. M. Ocko, X. Z. Wu, E. B. Sirota, S. K. Sinha, O. Gang, and M. Deutsch, *Phys. Rev. E* **55**, 3164 (1997).
- [4] G. A. Sefler, Q. Du, P. B. Miranda, and Y. R. Shen, *Chem. Phys. Lett.* **235**, 347 (1995).
- [5] T. Pfohl, D. Beaglehole, and H. Riegler, *Chem. Phys. Lett.* **260**, 82 (1996).
- [6] J. J. Jasper and E. V. Kring, *J. Phys. Chem.* **59**, 1019 (1955).
- [7] H. Gang *et al.*, *Europhys. Lett.* **43**, 314 (1998).
- [8] A. V. Tkachenko and Y. Rabin, *Phys. Rev. Lett.* **76**, 2527 (1996); E. B. Sirota, X. Z. Wu, B. M. Ocko, and M. Deutsch, *Phys. Rev. Lett.* **79**, 531 (1997); A. V. Tkachenko and Y. Rabin, *Phys. Rev. Lett.* **79**, 532 (1997); Y. Hayami and G. H. Findenegg, *Langmuir* **13**, 4865 (1997).
- [9] E. B. Sirota and A. B. Herhold, *Science* **283**, 529 (1999), and references therein.
- [10] A. W. Adamson and A. P. Gast, *Physical Chemistry of Surfaces* (John Wiley & Sons, Inc., New York, 1997), 6th ed.